LA-UR -84-1835

Los Alamos National Laboratory is operated by the University of California for the United States Department of Energy under contract W-7405-ENG-36

TITLE SPACE NUCLEAR POWER SYSTEM AND THE DESIGN OF THE NUCLEAR ELECTRIC PROPULSION OTV

LA-UR--84-1835

DE84 014395

AUTHOR(S) D. Buden, ES-NP
P. W. Garrison, Jet Propulsion Laboratory

SUBMITTED TO AIAA/ASME/SAE 12th Joint Propulsion Conf., Cincinnati, OH, June 11-13, 1984

Los Alamos National Laboratory
Los Alamos, New Mexico 87545

FORM NO. 836 R4
ST. NO. 2629 5 81

SPACE NUCLEAR POWER SYSTEM AND THE DESIGN OF THE NUCLEAR ELECTRIC PROPULSION OTV

D.Buden*
Los Alamos National Laboratory

P.W. Garrison**
Jet Propulsion Laboratory

Abstract

Payload increases of three to five times that of the Shuttle/Centaur can be achieved using nuclear electric propulsion. Various nuclear power plant options being pursued by the SP-100 Program are described. These concepts can grow from 100 kW_e to 1MW_e output. Spacecraft design aspects are addressed, including thermal interactions, plume interactions, and radiation fluences. A baseline configuration is described accounting for these issues. Safety aspects of starting the OTV transfer from an altitude of 300 km indicate no significant additional risk to the biosphere.

I. Introduction

The mission envisioned here for nuclear electric propulsion is that of raising satellites from low Earth orbit (LEO) to geosynchronous Earth orbit (GEO). Orbit raising could be performed for one-way missions, where the power supply is also the electric source for the satellite, or as round-trip missions, where a delivery vehicle is brought back for future missions.

Nuclear electric propulsion (NEP) systems are optimized by constructing low-mass nuclear power plants. Electric power levels of one hundred kilowatts up to several megawatts are desirable. Desirable goals for the power plant specific mass range from 20-30 kg/kW at the lower powers to 5-10 kg/kW at the higher powers.

Several different reactor power systems concepts are candidates for space power systems. Under the Space Nuclear Reactor Systems Technology (SP-100) Program, the field has been narrowed to three concepts for 100 kW_e. Growth versions to the megawatt range are possible. The selected candidates include a high-temperature (1500 K) fuel-pin reactor with thermoelectric power conversion, an in-core thermionic reactor power system, and a lower-temperature (~ 900 K), fuel-pin reactor with Stirling power conversion.

The design of an NEP spacecraft requires consideration of a wide range of subsystem interactions. In addition to the usual thermal and plume interactions, NEP orbital transfer vehicles (OTV) designs must address the reactor neutron and gamma fluxes, the electromagnetic fields produced by the electric propulsion subsystem, and the natural radiation associated with the low-thrust trajectory.

Electric thruster interactions with science and telecommunications can be a serious problem and are complicated by the long periods of thruster operation required. The NEP spacecraft thermal design is dominated by the large, high temperature radiator that is required to reject the power system waste heat.

Studies conducted since the early 60's have developed a variety of NEP stage configurations. These configurations and a configuration recently developed for the 100 kW_e SP-100 nuclear power system are discussed. The performance of a nuclear electric propulsion system in maneuvering from LEO to GEO as a function of flight times, payload and reactor power levels has been calculated. Assuming a 120-day orbit transfer, 19,000 kg can be moved from LEO to GEO in a single Shuttle trip with a 400 kW_e power system. Significant payload gains are achieved over chemical stages, where the Inertial Upper Stage can deliver 2270 kg and the Centaur up to 6360 kg.

II Orbit Transfer Between LEO to GEO

The potential application of nuclear power to rocket propulsion was recognized early. The energy available from a unit mass of fissionable material is approximately 10^7 times larger than that available from the most energetic chemical reaction. Approxi-

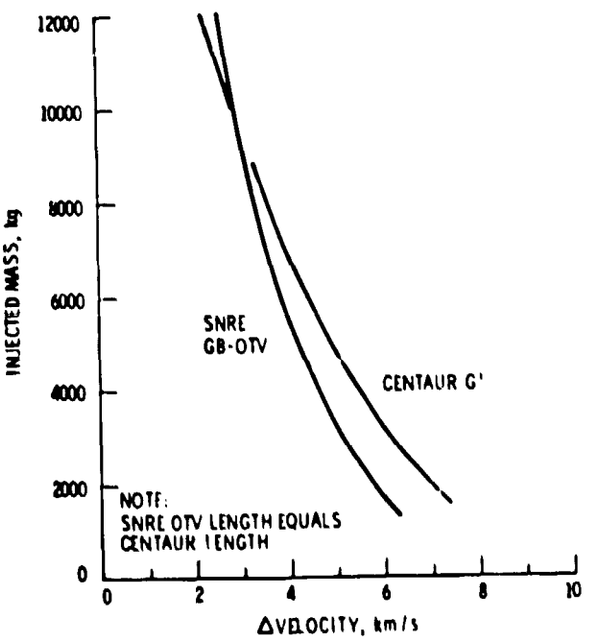

Fig. 1. Chemical and SNRE OTV performance based on Centaur G' length (ground based).

*Manager for Special Energy Conversion Projects, Member AIAA.
**Supervisor of Propulsion System Analysis Group, Member AIAA.

mately $3B was invested in solid core nuclear rocket development in the U.S. prior to 1973. This work was principally directed at the development of large, high-thrust engines based on hydrogen-cooled graphite reactor technology. The Nuclear Engine for Rocket Vehicle Application (NERVA) that resulted from this program was designed and operated at 1100 MW with a thrust of 333 kN. A Small Nuclear Rocket Engine (SNRE) was designed by Los Alamos National Laboratory for unmanned OTV and planetary mission applications. This 370 MW engine was designed for a thrust of 73 kN and a specific impulse of 875-975s. Fig. 1 shows a comparison between the performance of the SNRE-OTV and that of a Centaur G', both constrained to a single shuttle launch. The impulsive ΔV requirement for a LEO-GEO transfer is approximately 4200 m/s for a one-way mission and 8400 m/s for a round trip mission. It is clear that the higher specific impulse of the SNRE is insufficient to offset the lower propellant mass fraction of the hydrogen fueled SNRE-OTV stage when constrained to a single shuttle launch. The relaxation of this constraint permitted by space basing the OTV is addressed by Fig. 2. Here the Centaur G' is fully loaded and the SNRE-OTV is sized such that its resupply requirements are equal to those of the Centaur.

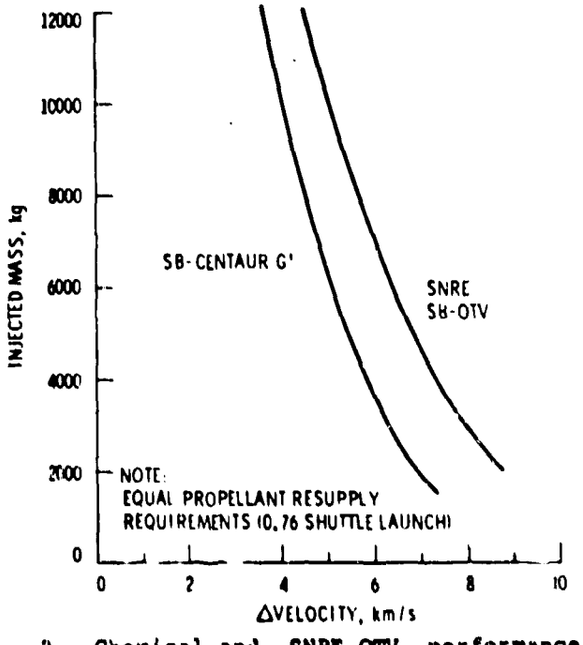

Fig. 2. Chemical and SNRE OTV performance based on fully loaded Centaur G' (space based).

The subject of this paper is the nuclear electric propulsion OTV. In this concept the nuclear reactor is a heat source for one of a variety of the 1 to electric power conversion processes. The electrical power produced is supplied to one of several electric propulsion systems, examples of which include resistojets, arc jets, ion thrusters and magnetoplasmadynamic (MPD) thrusters. Candidate propellants for these systems include liquid metals (e.g., Hg and Cs), inert gases (e.g., Ar and Xe) and hydrogen. Nuclear electric propulsion (NEP) systems provide higher specific impulse and lower thrust than a chemical propulsion system of the same mass. Jet power (W) can be expressed as the product of specific impulse, I_{sp} (S), and thrust, F (N),

$$P = \frac{gFI_{sp}}{2\eta}$$

In this equation η is the conversion efficiency and g is 9.8 m/s^2. Chemical rockets output prodigious quantities of power for short periods of time. The two RL-10 engines of the Centaur produce a total of 287 MW. The jet power delivered by nuclear electric propulsion system cannot exceed the electrical power output of the nuclear electric power supply (100 kW_e - 1 MW_e for the OTV's considered in this paper). Therefore the maximum thrust (η = 1.0) that can be produced at a specific impulse of 1000s is 20-200 N and at 5000s is 4-40 N. NEP OTV's are therefore low acceleration vehicles that require trip times many times greater than those of chemical OTV's but deliver signficantly more payload per unit mass of propellant expended. As is the case in terrestrial transportation systems, there will be a requirement for both the rapid delivery of time schedule critical materials and the economic delivery of heavy payloads including bulk materials. It is the latter requirement as well as that of transporting acceleration limited structures that the NEP-OTV is best suited to serve.

Many previous studies of NEP for orbit raising applications have been conducted. The objective of this paper is neither to provide an exhaustive review of this body of literature nor to develop a new approach to the design of a NEP-OTV. The objective is to provide an overview of nuclear electric power and propulsion system options for the OTV application. In so doing, we have to shed some light on the special problems associated with the integration of NEP into a practical OTV design and to illustrate to first order the performance of NEP-OTVs relative to that of chemical OTVs.

Data for selected electric propulsion systems are given in Table I[1] The performance of the nuclear electric propulsion (NEP) OTV is

TABLE I

DATA FOR ELECTRIC PROPULSION VEHICLES

Device	Specific Impulse (sec)	Total system efficiency (%)	Tankage fraction (%)	Thruster size	System Power (kW_e)	Propulsion System Mass (kg)
NH_3 arcjet	1000	40	15	30 kW_e	100	500
				50	300	1500
				80	600	3000
				30	1000	5000
Hg ion thruster	3000	60	5	30 cm	100	1360
				50	300	3940
				80	600	3640
				50	1000	5670
Hg ion thruster	5000	70	5	30 cm	100	940
				50	300	2670
				80	600	3860
				50	1000	4500

presented in Fig. 3[1] based on the assumption that the nuclear power supply is part of the payload. This is an appropriate assumption for missions which require the large amount of electrical power provided by the reactor for on-orbit operations. Figure 3 indicates that a transit time of 120 days can be achieved by a 400 kW_e OTV with a payload of 19000 kg.

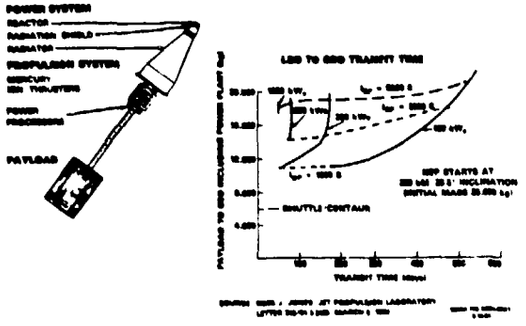

Fig. 3. Shuttle/Nuclear Electric Propulsion to GEO.

Table II[1] compares the payloads and transit time of the Centaur with that of the 400 kW_e NEP OTV. For Shuttle/Centaur the maximum payload mass is about 6000 kg to GEO. Assuming half the payload mass is assigned to the power system and that a solar dynamic system is used to represent future solar power technology, one could deploy a 40 kW_e power system. This leaves a balance-of-payload of 3000 kg.

Projected performance of nuclear power plant systems is given in Fig. 4. Nuclear reactor power systems mass and specific mass change non-linearly as a function of power level. The reasons for this are: (1) reactors must be designed to have a critical fuel mass; small incremental fuel additions will lead to larger gains in power output (increasing reactor mass 40 percent will double power output); (2) shielding is an exponential function of thickness (doubling reactor power leads to about a 33 percent increase in shield mass); and (3) the mass of thermoelectric converters tends to be linear with power output, but dynamic converters are not. The mass and specific mass curves include radiation attenuation shielding for un-manned payloads (i.e. electronics).

TABLE II

COMPARISON BETWEEN CENTAUR AND 400 kW_e NEP OTV PERFORMANCE

	Shuttle/Centaur	Shuttle/NEP (400 kW_e) [2] Power plant part of payload	Power plant part of expendables	Power plant part of expendables & payload
Total Power/payload Power	40/40[1]	400/400	400/8	400/16
Bal-of-payload (kg)	3000	10,000	12,000	15,000 [3]
Transit time (days)	0.25	120	120	120

(1) Solar-dynamics
(2) Assumed spacecraft long-term power need is 40 kW_e and nuclear power plant mass is 3000 kg.
(3) 400 kW_e power plant mass = 6000 kg.

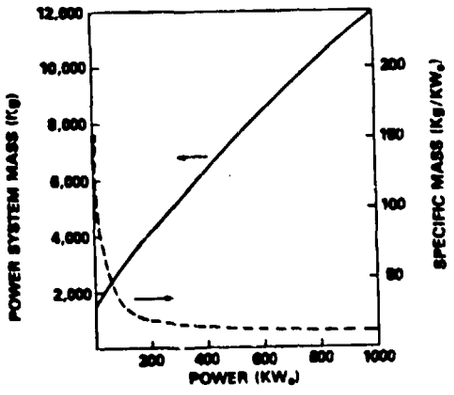

Fig. 4. Space nuclear reactor power system performance projections.

Based on Fig. 4, the mass of the 400 kW_e power plant is 6000 kg. For missions not requiring this power, the mass of the power plant must be subtracted from the payload shown in Fig. 3 to give a payload of 13,000 kg for these missions. If the spacecraft needs 40 kW_e for the payload (the amount a solar dynamic system was computed to be able to deliver), we can charge the equivalent nuclear power plant mass to the spacecraft and the balance to the propulsion system. The payload balance is 15,000 kg. The latter payload is five times the payload in a spacecraft containing a solar dynamic power system delivered by a Shuttle/Centaur transportation vehicle. Though 3-4 months are added to the transfer times from LEO to GEO, the total mission schedule may not be impacted when one considers that several Shuttle launches and on-orbit assembly are eliminated.

A manned NEP OTV does not appear reasonable at this time because of the added radiation shielding that would be required (10,000-15,000 kg) and the relatively long transit times. The unmanned tug would require resolution of such issues as: (1) a manned, shielded docking port in LEO and perhaps GEO; (2) safety of large fission inventories on the return to LEO; (3) possible separation of the nuclear reactor or power systems during maintenance of the remainder of the vehicle and refueling of the electric propulsion tanks; and (4) long-term scheduling with perhaps two round trips per year.

III. Nuclear Power Systems

Following screening of over a hundred potential space nuclear power system concepts by the SP-100 program, the field has now been narrowed to three candidate systems which appear to meet the requirements in Table III with a reasonable balance of technical risks and development time.

One concept uses a fast spectrum, lithium-cooled, pin-type fuel element reactor coupled to thermoelectrics for power conversion (Fig. 5) (2). The system is made up of a 12 sided cone structure with a 17 degree cone half angle. The reactor, which is a right

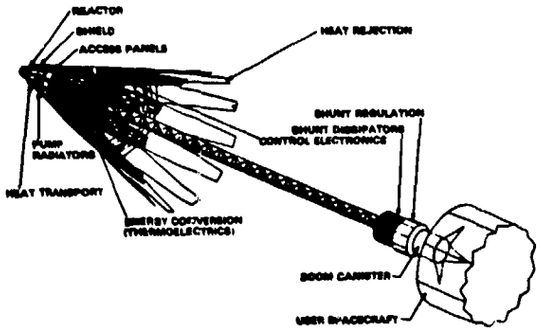

Fig. 5. High-temperature reactor with thermoelectric power conversion concept.

circular cylinder, approximately one meter in diameter and one meter high is at the apex of the conical structure. It is controlled by twelve rotatable drums each with a section of absorbing material and a section of reflective material to control the criticality level. Control of the reactor is maintained by properly positioning the drums.

The shield is mounted directly behind the reactor and consists of both a gamma and a neutron shield. The gamma shield consists of multiple layers of tungsten designed so as to prevent warping. The neutron shield is made up of a series of axial sections with a thermal conductor between the axial sections. The thermal conductor carries the gamma and neutron generated heat to the shield surface where it is radiated to space. Anticipated temperature levels are 675 K maximum.

Thermal transport is accomplished by a lithium working fluid which is pumped by a thermoelectrically driven EM pump. The thermoelectrics for the pump are powered by the temperature drop between working fluid and the pump radiators. This approach assures pumping of the working fluid as long as the reactor is at temperature and facilitates the cool down of the reactor when power is no longer required. The reactor thermal interface with the heat distribution system is through a set of heat exchangers. In this way, the reactor system is self-contained, can be fabricated and tested at a remote facility, and can be mated to the power system down stream. Access panels are provided on the main body to facilitate the assembly of the heat distribution system to the heat exchangers.

Thermoelectric elements are bonded to the internal surfaces of the heat rejection panels and accept heat from the source heat pipe assembly. The design for the thermoelectric is a bi-couple using boron carbon (p-type) and lanthanum sulfur (n-type) elements. The heat rejection surfaces are beryllium sheets with titanium potassium heat pipes brazed to the surface to distribute and carry the heat to the deployable panels which are required to provide additional heat rejection surfaces. The deployable panels are thermally coupled through a heat pipe to heat pipe thermal joint which is very similar to the source heat pipe to heat exchanger joint, made integral by the use of special self-brazing materials for self-brazing in orbit. In order to allow the deployment of the panels, a bellow-like heat pipe section is mounted at the tail end of the heat pipes on the fixed panel. Such a flexible heat pipe has been demonstrated.

The system has a wide range of flexibility. Its output can be expanded either by increasing the thermoelectric figure-of-merit or by an increased size and weight of the system. A map of potential scalability of the system is shown in Fig. 6.

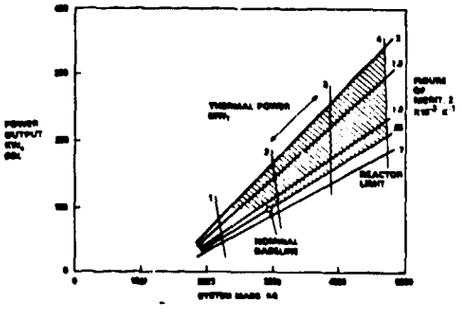

Fig. 6. High-temperature reactor with thermoelectric conversion concept scalability.

A second approach is an in-core thermionic system with a pumped sodium-potassium eutectic coolant. The general arrangement of the in-core thermionic space power system design is shown in Fig. 7 (3). The design forms a conical frustum that is 5.8m long with minor and major diameters of 0.7m and 3.6m respectively. The reactor converter subsystem includes: the reactor, the reflector/control drums, and the neutron shield. The reactor contains the thermionic fuel element (TFE) converters within a cylindrical vessel, which is completely surrounded by control drums. The NaK primary coolant routing to and from the reactor vessel are arranged so that the hot NaK leaves the reactor at the aft end and the cold NaK is returned to the forward end, thus helping to minimize differential thermal expansion in the piping. The reactor is also surrounded by an array of long, thin cylindrical reservoirs which collect and retain the fission gases generated in the

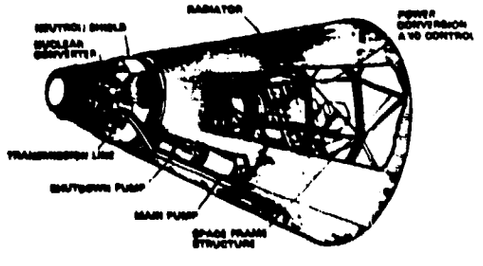

Fig. 7. In-core thermionic power plant concept.

reactor core during the operating life of the system. Waste heat is removed from the primary reactor loop through the heat exchanger. The energy is transferred through the heat sink heat exchanger to heat pipes that form the radiating surfaces for rejection of heat to space.

Within the reactor vessel are: 176 TFEs, a grid plate to support TFEs at one end, a tungsten gamma shield, and eutectic NaK coolant. Each TFE is welded into the flat top head of the vessel, but allowed to move axially in the grid plate, which restrains radial movement. Differential axial expansion is expected to be small, since the TFE sheath tubes and reactor vessel are both of Nb-1% Zr alloy, and their temperatures are nearly the same.

The TFE consists of six cells connected in series with end reflectors of BeO. Boron carbide neutron absorber is placed at both ends of the fuel element to reduce the thermal neutron flux in the coolant plenums and in the gamma shield and neutron shield. This reduces activation of the coolant, secondary gamma ray production, and nuclear heating of the lithium hydride shield.

The individual cells, see Fig. 8, are connected in series to build up voltage from the 0.4 V cell output. Electrical power is generated in the space between the tungsten emitter and niobium collector, and the electrical current output is conducted from one cell to the next through the tungsten stem of the emitter and the tantalum transition piece. The UO_2 fuel is held in place and supported during launch by a retention device designed to retract when the fuel expands on heating. The alignment spring at the base of the emitter centers the emitter in the collector to maintain a uniform interelectrode spacing. It also restrains the emitter against launch vibration to prevent large displacements and limit stresses in the thin stem at the other end of the emitter.

Fission gases are vented from the UO_2 fuel to prevent the build-up of pressures that would cause creep deformation of the tungsten emitter and close the interelectrode space. Fission gases are kept separate from the cesium by the ceramic-to-metal seal and the arrangement of passages through the emitter cap and transition piece.

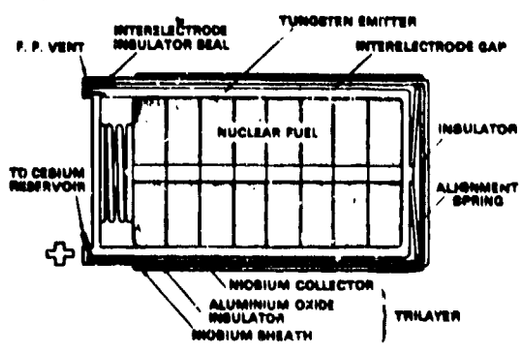

Fig. 8. In-core thermionic converter.

Reactor control is provided by the rotation of the 20 cylindrical control drums surrounding the reactor.

The heat transport subsystem is a single loop that includes all of the NaK plumbing aft of the reactor, the heat sink heat exchanger, and the radiator. The 100 mm diameter NaK lines to and from the reactor are routed inside helical groves in the outer surface of the neutron shield and then passed along the inside surface of the radiator to connect to the heat sink heat exchanger. The configuration of the NaK lines along the shield is helical, rather than straight, to avoid degradation of the shield performance due to neutron streaming in the pipe channels. The helical channels in the shield are also occupied by the electrical transmission lines, which are flattened in cross-section and are routed over the NaK lines to serve as meteoroid protection.

Electromagnetic pumping is used to circulate the NaK during normal operation and during shutdown when residual NaK flow in the circuit must be maintained. Two electromagnetic pumps are provided in the cold leg of the NaK circuit: an annular linear induction pump serving as the main pump and a parallel thermoelectromagnetic pump (with a check valve) to provide shutdown pumping capability.

The radiator contains two finned-heat pipe panel assemblies, which form a conical frustum when the panels are assembled on the radiator structure. The heat pipes follow the slant height of the core and are deployed fore and aft of the heat sink heat exchanger, to which they are thermally coupled. The radiator also provides environmental protection for the equipment which it houses.

Growth is possible by either redesigning the reactor with more TFEs or increasing the emitter temperature. An upper temperature level of about 2000 K is believed to be an operational limit for the tungsten emitter.

TABLE III

SP - 100 GOALS

Performance	
Power output, net to user (kW_e)	100
Output variable up to 100 kW_e	
Full power operation (y)	7
System life (y)	10
Reliability (%)	
1st system, 2 y	0.95
Growth system, 7 y	0.95
Multiple restarts	
Physical Constraints	
Mass (kg)	3000
Ø (m, length within STS envelope (m)	6.1
Interfaces	
Reactor induced radiation after 7 y operation, 25 m from forward end of reactor	
Neutron fluence (n/cm^2)	5×10^{11}
Gamma dose (rads)	5×10^5
Mechanical	STS launch conditions
Safety	Nuclear Safety Criteria and Specifications For Space Nuclear Reactors

Fig. 9 shows growth projections for the current reactor design.

The third approach uses a Stirling engine to convert heat from a lower-temperature (900 K), fuel-pin reactor design to electricity. This design emphasizes the use of state-of-the-art fuel pins of stainless steel and UO_2 with sodium as the working fluid. Such fuel pins have been developed for the breeder reactor program with 1059 days of operation and 8.5% burn up demonstrated.

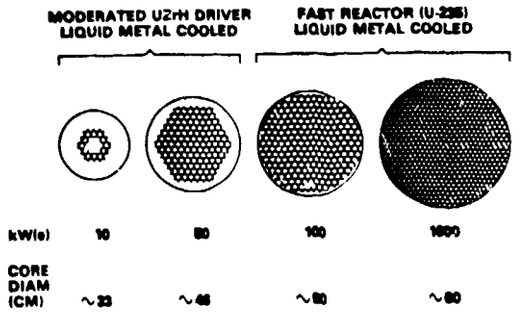

Fig. 9. In-core thermionic reactor size scalability.

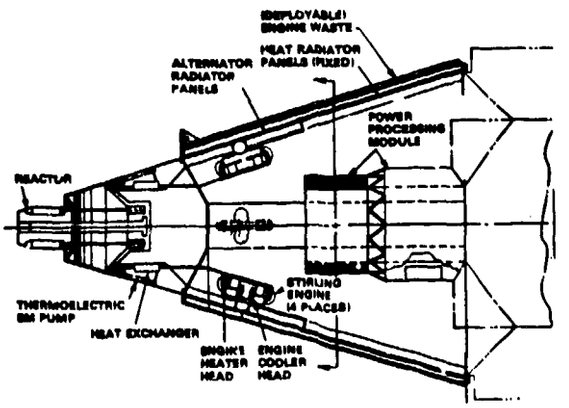

Fig. 10. Stirling engine conversion concept.

The reactor can be similar in design to the high-temperature reactor but utilizes lower temperature materials. In Fig. 10, (4) the reactor is constructed as a separate module from the conversion subsystem. Four Stirling engines, each rated to deliver 33 kW_e, are included in the design concept. This provides some redundance in case of a unit failure. Normally the engines operate at 75% of rated power to produce a 100 kW_e output. Each engine contains a pair of opposed motion pistons which operate 180 degrees out of phase. This arrangement eliminates unbalanced linear momentum. Each engine receives heat from a pumped loop connected to the reactor vessel. An alternate arrangement would deliver the heat through an interface heat exchanger with heat pipes between the heat exchanger and engine. The heat is supplied to heater heads integral with the engine. Waste heat is removed from the cooler heads and delivered to a liquid-to-heat pipe heat exchanger. The heat pipes, in turn, deliver the waste heat to the radiator where it is rejected to space.

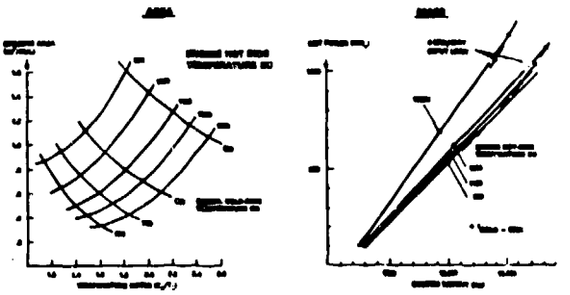

Fig. 11. Stirling power system concept scalability.

Fig. 11 provides performance curves for the Stirling system. A low temperature will meet the 100 kW_e goals. However, growth systems favor combining the Stirling engines with higher temperature reactors both to minimize mass and to reduce the heat rejection surface areas.

IV. NEP Spacecraft Interactions

Figure 12 identifies the subsystem interactions that distinguish the design of an NEP-OTV from that of a chemical OTV. Special attention must be given to the radiation and thermal environments produced by the power system and to the electromagnetic fields and propellant fluxes produced by the propulsion system.

NEP OTV designs must address the reactor neutron and gamma fluxes as well as the significantly larger natural radiation exposure that results from the increased time spent by the low thrust NEP OTV in transition through the earth's radiation belts. The NEP OTV transferring between LEO and GEO spends 100 to 300 days in the intense regions of these belts. Fig. 13 shows the cumulative radiation exposure during this phase of the mission and compares this exposure to that expected for the Galileo orbiter spacecraft. While the Jovian radiation environment is more intense than the Earth's, the Galileo

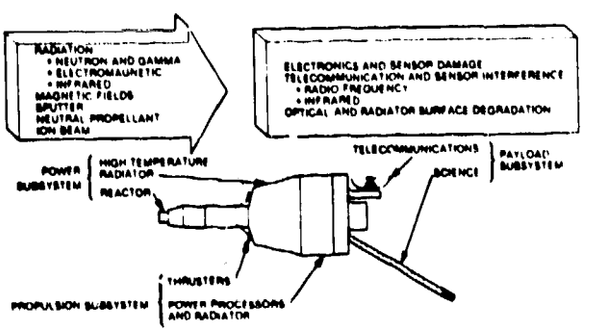

Fig. 12. NEP spacecraft subsystem interactions

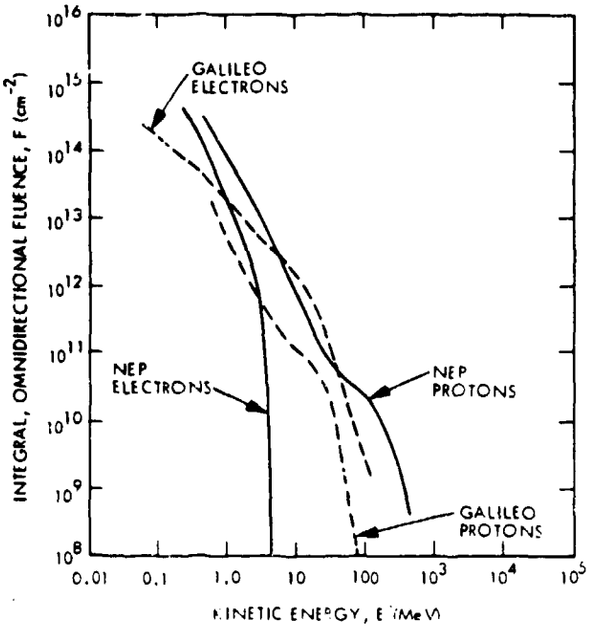

Fig. 13 NEP spacecraft radiation exposure during transit of Van Allen belts.

orbiter spends most of the time outside the radiation belts, and thus the radiation exposures are comparable to those seen by the NEP OTV in transferring between LEO and GEO. Radiation shielding, roughly equivalent to that required for the Galileo spacecraft (0.5 cm aluminum) must be provided to protect the NEP OTV avionics and payload from the natural radiation environment. These shielding requirements should be considered when comparing the performance of chemical and nuclear electric propulsion vehicles.

Reactor produced neutron and gamma radiation effects on OTV and payload systems are controlled by a combination of shielding and spatial separation between the reactor and critical components. The radiation limits for the Galileo spacecraft are 7.5×10^4 rads and 2.5×10^{10} N/cm^2(1 MeV). Shield design criteria currently being used in the SP-100 Program (5×10^5 rads and 10^{13} N/cm^2) are significantly higher than these values based on projected advances in radiation hard electronics technology. If the imposition of such requirements on general purpose OTV payloads is not practical, additional shielding will be required. The radiation shield is a significant fraction of the power subsystem mass, approximately 30% for a 100 kW$_e$ system and 10% for a 10 MWe system. These estimates are representative of shadow shields which intercept a small fraction of the reactor fluence. OTV systems such as thrusters, booms and radiators located outside the protected zone are not only themselves subject to radiation damage but serve to increase the fluence to systems located behind the shield by scattering radiation into these regions. Such configurations should be avoided. A space-based NEP OTV will require additional shielding on the vehicle or at the depot to permit access for maintenance and servicing.

The thermal design of the NEP OTV is complicated by the large, high temperature radiators required for heat rejection by the power and propulsion power processor systems. The thermal power rejected is typically 4 to 15 times the electrical power supplied to the thrusters. Power system radiators must operate at high temperatures (700-1000K) to keep the surface area and mass of the radiator within acceptable bounds. Propulsion system power processor heat rejection requirements vary depending on the electric propulsion system used, but are much lower than those of the power system and can be met with radiators operating at lower temperatures (300-400K). The integration of these large, high temperature surfaces into the spacecraft configuration requires considerable ingenuity to avoid excessive thermal loads to the OTV propellants and payload electronics. Advanced, lightweight radiator concepts, such as the droplet radiator, may permit operation at lower temperatures but these radiators introduce additional design and operational constraints. The use of cryogenic propellants, such as argon or hydrogen, will likely require sophisticated thermal control systems to prevent excessive boiloff.

Various interactions can occur between the electric propulsion system and spacecraft surfaces and systems. These interactions vary depending on the type of thruster used (e.g., ion, magnetoplasmadynamic (MPD), arcjet, or resistojet) and the propellant (e.g., mercury, argon , xenon, or hydrogen). The following discussion focuses on the electron bombardment ion thruster since the characteristics of this thruster are better defined than those of other electric thrusters. Four basic mechanisms characterize electric propulsion/spacecraft interactions; 1) surface erosion, 2) film deposition, 3) plasma interactions, and 4) electromagnetic interference.

Spacecraft surfaces exposed to the ion thruster beam plasma can be eroded. Such erosion can result in the failure of structural members, the optical degradation of thermal control surfaces and spacecraft contamination by the sputtered material. Thruster location should be selected to avoid impingement of the beam plasma on spacecraft surfaces. The half angle of the energetic beam can be as large as 40° for some thrusters, but is typically 15°.(5)

The deposition of propellant and non-propellant films on critical spacecraft surfaces can be a serious problem. The non-propellant efflux is composed of material sputtered from thruster components such as the neutral accelerator grid. Such materials can be transported upstream of the thruster by diffusion and electromagnetic field effects. The deposition of these materials on surfaces depends on the vapor pressure of the materials and the temperature of the surfaces. Non-propellant materials such as molybdenum and propellants such as mercury with low vapor pressures will accumulate on

all but the highest temperature surfaces. No deposition should occur on the power and propulsion system radiators. Thin films of these materials can alter surface electrical conductivity and thermal radiation characteristics. Changes in surface electrical conductivity can impact the performance of photovoltaic arrays, antennas and electrical insulators; changes in surface thermal properties can impact radiator performance. Propellants such as argon, xenon and hydrogen have much higher vapor pressures and will not pose a contamination problem.

Interactions between the NEP-OTV, the ambient space plasma, and the electric propulsion generated plasma can result in spacecraft charging and arcing which can produce upsets in logic circuits, breakdown of electrical insulation, and enhancement of surface contamination. Such effects are of principal concern with power system thermoelectric elements and interconnects. (5) Spacecraft electrostatic potential can likely be controlled during thrusting by beam neutralization but this problem requires further study.

Electromagnetic interference is produced by the ion thruster discharge chamber permanent magnets and dynamic electromagnetic fields. The transmission of radio signals through the ion beam has been investigated by JPL. (6) S-band transmission through the beam of a 2-amp, 30-cm mercury ion thruster showed only a small amount of signal attenuation and negligible reflection loss. These experiments were not extended to X-band or inert gas propellants; but the effects at that frequency should be significantly smaller and the inert gas plasmas should (to first order) behave the same as the mercury plasma in terms of absorption and reflection of RF signals.

Numerous NEP spacecraft configurations have been proposed. (7,8) Fig. 14 presents a configuration developed for an early SP-100 power system concept. (9) This configuration serves to illustrate the impact of previously discussed NEP interactions on vehicle design. In this configuration the thrust vector is orthogonal to the vehicle longitudinal axis and the reactor and payload are located at the opposite ends of the vehicle. The side thrust/end reactor configuration was selected because this design avoids many of the less well defined subsystem interactions (e.g., sputter erosion of hardware downstream of the thrusters and the scattering of nuclear radiation by hardware not protected by the shadow shield). Clear fields of view are provided for the high temperature power system and thruster system power processor radiators. Thermal control problems are minimized by integrating the spacecraft subsystems along the thermal gradient, i.e., high temperature systems, and low temperature are located on opposite ends of the spacecraft and intermediate temperature systems are located in between. The design also provides a clear field of view for payload systems.

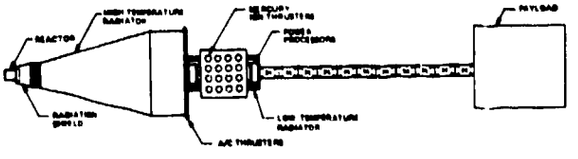

Fig. 14 SP-100 NEP OTV flight configuration

Ion thruster technology was used for propulsion. The thrust subsystem power processor packages are structurally integrated with two flat plate radiators which reject processor waste heat at 320 K. The sixteen individual gimbaled 30 cm thrusters shown in this configuration are attached to a support structure which is integrated into the power processor radiator structure. A propellant tank is located at the spacecraft center of gravity (CG), behind the thrusters and between the two banks of power processors. Mercury, xenon and argon are potential propellants. The inert gases may be preferable for the OTV mission due to potential mercury contamination of earth's atmosphere, however, mercury is preferred for the planetary missions due to ease of storage and better thruster performance. Mercury is also effective in reducing the radiation fluence to the payload.

The maximum length of the launch configuration of the spacecraft is limited by shuttle cargo bay dimensions. After leaving the cargo bay, the payload section of the spacecraft is extended 11 m from the end of the thrust module by a lightweight collapsible mast. This is necessary to place the spacecraft center-of-mass at the center of the main propellant tank (no CG change during burn). The extension also serves to place payload electronics at a distance (25 m) from the SP-100 shield consistent with the shield design requirement.

V. Safety Issues

Safety concerns are a major factor in design and operation of reactors for space power. To protect the Earth's population against undue risk, radiation levels at the time of a nuclear reactor reentering the Earth's atmosphere should be low. Most fission products decay away, if the orbital lifetime of a satellite in orbit is sufficiently long. A long-lived, high orbit is defined in the reactor safety specification (10) as an orbit with a liftime of 300 or more years. This corresponds to an initial altitude of about 750 km. Fig. 15 plots the radioactivity for a two megawatt-thermal reactor as a function of operating times (calculations were performed on the Origen code); Fig. 16 plots the orbital lifetimes as a function of altitude and the ballistic characteristics of the system. A cylindrical reactor reentering the atmosphere would fall near the upper

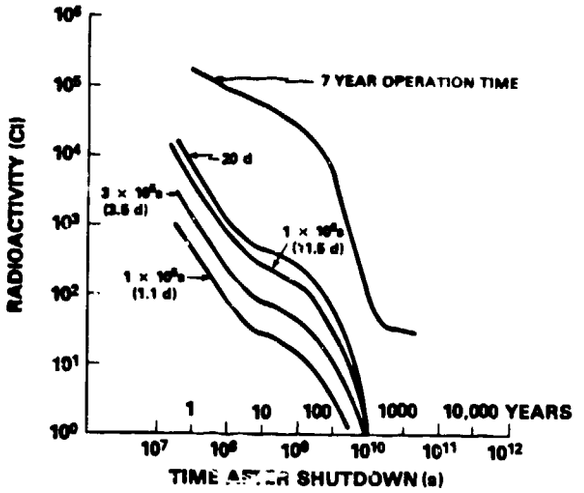

Fig. 15 Two megawatt thermal radioactivity decay.

curves, a space station would fall near the lower curves. The radioactivity calculations show that if the reactor reenters the biosphere after 300 years in orbit the fission product activity has been reduced from approximately 10^7 Ci to about 100 Ci.

Actinides are another source of radiation. Their quantity is proportional to the operating time, fuel enrichment, and reactor spectrum The dominant actinide is 239 Pu, which has a half-life of 24,390 y. At low thermal powe. and operating times, the actinide levels are very small; but at two megawatt-thermal power operating for seven years, they represent a four Ci radiation source.

Certain designs may use materials that are activated while in the reactor, such as Nb-1% Zr-0.1% C fuel cladding. Their presence can result in the generation of additional long-lived radioactive isotopes. For the reactor in reference 4, activation of the fuel cladding results in an increase of 22 Ci at the end of 300 y because 94 Nb is generated (half-life of 2×10^4 y).

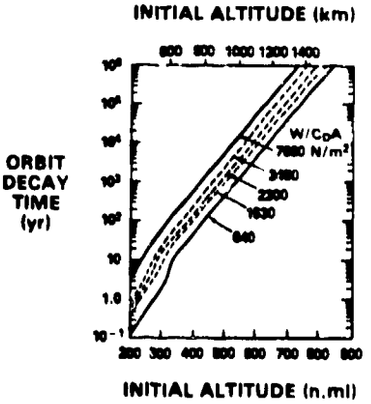

Fig. 16 Orbital decay times

The total dose level after 300 y is 118 Ci. It is derived mainly from long-lived isotopes. If the orbit time is increased to 600 y, the dose level decreases to 34 Ci and in 2000 y to 28 Ci.

To avoid payload penalties with the Shuttle, one would prefer an initial operational orbit at about 300 km. A 750 km orbit, corresponding to about a 300 y orbital lifetime, can be reached with shuttle by adding two OMS KITS; however this results in a 34% payload reduction. Safety questions associated with starting at 300 km altitude relate to: (1) the quantity of additional fission products present at reentry if an abort occurs prior to reaching a 300 y orbit; (2) the biological hazards of those fission products; and (3) whether the spacecraft can be powered into the atmosphere. The last condition can be avoided by independent and redundant control of the propulsion and power supply to insure NEP cut off if the spacecraft trajectory is unacceptable. The first two questions will be addressed.

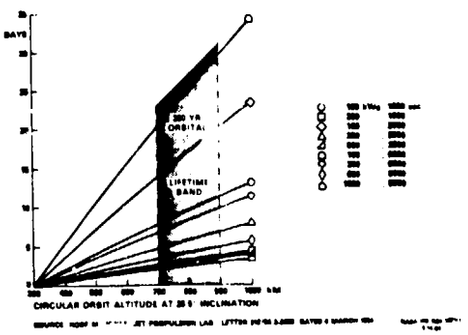

Fig. 17 Transit time from 300-1000 kM on trips to GEO.

NEP OTV trajectory data are presented in Fig. 17 for a range of powers and specific impulses(1) Aborts were assumed at various times during orbit transfer and the radiation levels compared with a 300 y orbit (Table IV). It was concluded that for a short duration of time the fission products could be greater than those produced by long term operation followed by a 300 y radioactive decay period. For 100 kW_e - NEP systems, the radiation levels above those for our reference case is several weeks for a 5000 s specific impulse and it is about one day for an 1000 s. The peak level for 1000 s is about 800 Ci.

If a more efficient electrical conversion subsystem is used with the 2 MW_t heat source, 400 kW_e output power can be achieved. Higher power reduces the time where radiation levels at reentry are above the 300 y orbit levels following an abort. For 400 kW_e this is less than one day for an I_{sp}=1000 s and 3.5 days for I_{sp}=5000 s. The radiation levels are such as to conclude that reactors designed to disperse on reentry could be started on a NEP transfer from below the 300 y orbit with little additional safety risk or damage to the biosphere.

The distribution of radioactive elements at several points in Table IV were reviewed. The results, Table V, indicate some build up in bone-seekers above the 7 y reference but does not change our conclusions.

TABLE IV

REENTRY RADIATION LEVELS FOR ABORTED NEP MISSIONS STARTING FROM 300 km ORBIT

(2 - MW_t Reactor)

100 kW_e NEP

Boost Time	Orbit Decay Time (y)			Radiation Levels at Reentry (Ci)		
Days	I_{sp}=1000s	3000s	5000s	I_{sp}=1000s	3000s	5000s
1.1	0.7	0.7	0.6	800	1.0×10^3	1.0×10^3
3.5	3	1	0.6	255	1207	3.0×10^3
11.5	3000	40	7	[.06]	[115]	326

400 kW_e NEP

Boost Time	Orbit Decay Time (y)			Radiation Levels at Reentry (Ci)		
Days	I_{sp}=1000s	3000s	5000s	I_{sp}=1000s	3000s	5000s
1.1	3	0.8	0.7	[86]	580	800
3.5	700	40	6	[0.5]	[35]	[110]
11.5			3000			[0.06]

[ ] Radioactivity dose levels below those after 300 y following 7 y operation.

TABLE V

RADIOACTIVE ELEMENTS ABSORBED BY HUMAN BODY (Ci)

(Two-Megawatt-Thermal)

	7 y operation 300 y orbit	1.1 d operation 3 y orbit	3.5 d operation 3 y orbit
Bone-seekers (Sr, Y, Zr, Nb, Ba, La, Pr, Nd, Pm)	40	46	138
Thyroid-seekers (I)	--	--	--
Kidney-seekers (Ru)	--	3	8
Muscle Tissues (Cs, Ba)	30	14	41
Total all radioactivity	118	86	255

VI. Summary

It appears that about 400 kW_e would be a desirable choice for NEP applications. Lower power significantly increases the transit times and higher power decreases the payload. Current 100 kW_e designs being pursued in the growth versions of SP-100 Program can deliver power plants using either in-core thermionics or a high temperature pin-fuel reactor with Stirling power conversions at 400 kW_e.

A NEP spacecraft concept has been developed with the thrust vector orthogonal to the vehicle longitudinal axis and the reactor and payload located at opposite ends of the vehicle. This configuration avoids such issues as sputter erosion and radiation scattering, and takes into account thermal interactions. Also, it allows for a clear view for payload systems.

Safety issues associated with starting NEP operations from 300 km are not significantly different than starting from a 300 year (750 km) orbit.

References

(1) Jones, R.M., Jet Propulsion Laboratory, Personel Communication, March 1984.

(2) R. Katuski, A. Josloff, A. Kirpech, F. Florio, "Evolution of Systems Concepts For a 100 kW_e Class Space Nuclear Power System," First Symposium on Space Nuclear Power System, Univ. of New Mexico, to be published Summer 1984.

(3) "Conceptual Design Studies in Support SP-100 Program," GA Technologies and Martin Marretta, La Jolle, CA, Report No. GA-C17354, Dec. 9, 1983.

(4) "SP-100 Conceptual Design Study" General Electric Co., Valley Forge, PA, Doc. No. 835SDS4262, Dec. 7, 1983.

(5) Deininger, W. D., "Electric Propulsion Produced Environments and Interactions with SP-100," JPL Report D-934, August 1983.

(6) Carruth, M. R., "Experimental and Analytical Evaluation of Ion Thruster/Spacecraft Interactions," JPL Report 80-92, January 1981.

(7) Philips, W. M., "Nuclear Electric Power System for Solar System Exploration," AIAA Paper 79-1337R, June 1979.

(8) "Nuclear Electric Propulsion Mission Engineering Study - Final Report," NASA-CR-131599 (Vol. I) and NASA-CR-131600 (Vol. II), March 1983.

(9) Garrison, P. W., Nock, K. T., "Nuclear Electric Propulsion (NEP) Spacecraft for the Outer Planet Orbiter Mission," AIAA Paper 82-1276, June 1982.

(10) "Nuclear Safety Criteria and Specifications For Space Nuclear Reactors," Dept. of Energy, Document OSNP-1, Rev.-0, Dated Aug. 1982, Washington, D.C.